Dynamic data analysis for pediatric airways

Chun-Wei Liu

Department of Computer Science,
University of North Carolina, Chapel Hill, NC
chunwei@cs.unc.edu

Abstract. The analysis of pediatric airway geometry using computed tomography (CT) images has provided rich diagnostic cues for doctors. Recently, dynamic CT data provides a better characterization of pediatric airways throughout the breathing cycle, for example to assess tracheomalacia. However, how to preprocess the increasing amount of dynamic data and how to analysis these data are still open questions. In this work, I performed dynamic data analysis using computer vision and machine learning approaches on synthetic and real airway data. In the future, I aim at building a 4D atlas for pediatric airways and to extend the approaches to other dynamic data modalities.

1 Introduction

The analysis of pediatric airway geometry using computed tomography (CT) image has provided rich cues for doctors to diagnose respiratory issue for patients. For example, given a 3D segmentation of CT image, doctors can diagnose tracheal stenosis by locating the position has smaller cross-sectional area in the airway and compare it to an normal control atlas [1].

Recently, dynamic CT data (4D CT) provides a better characterization of pediatric airways throughout the breathing cycle, for example to assess tracheomalacia, which is a disease of temporally collapse of partial airway. Comparing with spirometry, analysis on 3D CT image provides additional information about *where* the respiratory issue might cause. Then 4D CT image provides more information about *when* the respiratory issue might cause during the breath cycle.

However, how to preprocess the increasing amount of dynamic data and how to analysis these data are still open questions. While standard techniques for analysis 3D CT could be applied on analysis 4D CT in a frame-by-frame fashion, two major challenges can be addressed as follow. First, manually annotations or preprocessing cost of each subject has increased a factor proportional to the number of CT scans in a breath cycle. Second, no information sharing between time steps might cause temporal inconsistence for the analysis. In this work, I am going to address the above issues by performing dynamic data analysis using computer vision and machine learning approaches.

In Section 2, I will introduce the methods applying on pediatric airway analysis. Experiments on real airway data would be compiled in on Section 3. In Section 4, I will discuss the future works, including building a 4D atlas for pediatric airways and extending the approaches to other dynamic data modalities.

2 Methods

In terms of analysis subjects with huge varieties, data registration is an important step. Registration could be approached in different perspectives. First, registration on image, which uses image intensity as a major feature, has being developed in medical image analysis for past decade. Hill et al. and Sotiras et al. wrote very educated review articles on this topic [2, 3]. On the other hand, registration on shape, which uses geometric cues as major feature, has succeeded in many applications in computer vision and computer graphics fields [4, 5]. However, applying such techniques for aligning pediatric airway data was still a hard problem. Hong et al. proposed a simplified airway model which is much easier to register for further analysis [1].

2.1 Simplified airway model

In this work, I applied Hong et al.'s simplified airway algorithm. The algorithm first segments the airway from CT images using Otsu-thresholding and two manually chosen seeds that bracket the upper airway. Then the upper airway can be approximated by a centerline with cross sections. The centerline is inferred based on the heat distribution along the airway flow that is solved by a Laplace equation. Cross sections are cut from segmented airway geometry using planes that are orthogonal to the centerline. The area of the cross sections would be the 1D functional data representation of an airway.

2.2 Landmark detection

Once we have functional data, we can register them alone with some common landmarks across subjects. Typically the landmark annotation was performed manually. For reducing the manually annotation cost, based on Dalal and Triggs's detection framework [6], I propose a landmark detection framework using concatenating Histogram of Gaussian (HOG) features and geometric prior.

The first step in the framework is to train a binary classifier using concatenating HOG. HOG is well designed normalized local histograms of image gradient orientation in a dense sample grid. The original purpose of this feature was for human detection. Nevertheless, it captures edge or gradient structure that is very characteristic of local shape, and it can be efficiently computed. For applying HOG on 3D image, instead computing histogram is arbitrary 3D orientation, I attempted to computed 2D HOG in axial, coronal, and sagittal plane, which are the three perspectives for user annotations. This reduced the computational complexity and made learning feasible given limit amount of ground truth annotations. In prediction stage, the trained classifier can be applied to the particular landmark it was designed for. Figure 1 illustrated detection of trachea carina (TC).

After landmarks are located, we can register the functional data to the unified domain [7]. In Hong et al.'s original paper, each subject had five visible landmarks from nasal spine, choana, epiglottis tip, true vocal cord (TVC), and TC.

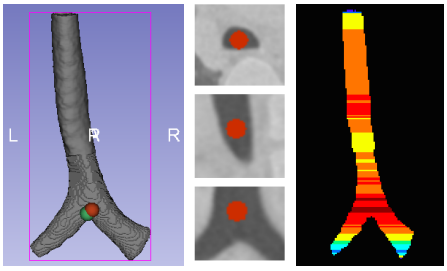

Fig. 1. Visualization of the framework of landmark detection. First, an airway geometry is segmented by Otsu-thresholding. Green marker is the ground truth annotation and red marker is the predicted location of TC. Second, concatenating HOG features are computed in the center of trachea in each depth. From top to down: Sagittal, coronal, and axial. Final, applying the trained classifier on these different hypotheses to get likelihoods of the landmark. Dark red indicates the highest likelihood of TC. In this case, the predicted TC has only 1.97 mm (the total length is 159 mm) away from the ground truth annotation. This error is only 1.2% of the entire airway.

In our dynamic data, most of subjects only have TVC and TC. Even thought, in some cases, TC is the only available landmark which makes alignment impossible using current approach. Then, a heuristic assumption would be applied to these special cases. The assumption is the subject has the same length of trachea from TVC to TC with the most relevant subject (in terms of age) in our data. Therefore, we can compute the portion of the existed trachea by measuring the ratio of the length of current trachea in physical space and the length of the most relevant subject from TVC to TC.

2.3 Statical atlas analysis

Given special aligned functional data I would like to capture population changes with respect to some factors, say age. A kernel regression approach can achieve the objective by assigning weights to data-object with respect to age. For example, I used Gaussian weight function $w_i(a_i; \sigma, \bar{a}) = c \exp(a_i - \bar{a})/2\sigma^2$, where a_i is the age for the observation i, σ is a predefined standard deviation and c is the normalization constant for fitting data to a specific age.

To further analyze the weighted data, I applied weighted functional boxplots to build statical atlas for each dynamic subject [8]. Functional boxplots was originally proposed by Sun and Genton [9] which requires a definition of band depth for functional data. Here I used a weighted version to fit the population changes.

Band depth is a rank of functional data for ordering it from the center outward. Basically, the idea is the more subsets to which a data is belonged, the more centrality that data might have. Given a set of functional data $Y = \{y_i | i = 1, ..., n\}$, a combinatorial function C which enumerates all two pair combinations

in a set, and a band function $B(y_1, y_2) = \{(t, x(t)) : t \in \mathrm{T}, \min(y_1(t), y_2(t)) \leq x(t) \leq \max(y_1(t), y_2(t))\}$, the band depth D of a functional data y with respect to a set Y can be defined as

$$D(y; Y) = \sum_{y_i, y_j \in C(Y)} I[y \subset B(y_i, y_j)], \tag{1}$$

where I is an indicator function. A general version of band depth is weighted modified band depth

$$D'(y; Y) = \sum_{y_i, y_j \in C(Y)} w_i w_j \lambda[B(y_i, y_j)] \tag{2}$$

where λ is the Lebesgue measure, and ws are the weights of kernel regression. The measurement of membership of a functional data is relax in (2), and it is based on a weighted populations which fits our objective.

When a rank of functional data is available, we can compute interesting statics such as median, interquartile range, and outliers of the population. I applied (2) to compute population atlas and plot subject dynamics upon the population atlas using (1).

3 Experiments

4 Discussion

References

1. Hong, Y., Davis, B., Marron, J., Kwitt, R., Singh, N., Kimbell, J.S., Pitkin, E., Superfine, R., Davis, S.D., Zdanski, C.J., et al.: Statistical atlas construction via weighted functional boxplots. Medical image analysis **18**(4) (2014) 684–698
2. Hill, D.L., Batchelor, P.G., Holden, M., Hawkes, D.J.: Medical image registration. Physics in medicine and biology **46**(3) (2001) R1
3. Sotiras, A., Davatzikos, C., Paragios, N.: Deformable medical image registration: A survey. Medical Imaging, IEEE Transactions on **32**(7) (2013) 1153–1190
4. Belongie, S., Malik, J., Puzicha, J.: Shape matching and object recognition using shape contexts. Pattern Analysis and Machine Intelligence, IEEE Transactions on **24**(4) (2002) 509–522
5. Li, H., Luo, L., Vlasic, D., Peers, P., Popović, J., Pauly, M., Rusinkiewicz, S.: Temporally coherent completion of dynamic shapes. ACM Transactions on Graphics (TOG) **31**(1) (2012) 2
6. Dalal, N., Triggs, B.: Histograms of oriented gradients for human detection. In: Computer Vision and Pattern Recognition, 2005. CVPR 2005. IEEE Computer Society Conference on. Volume 1., IEEE (2005) 886–893
7. Ramsay, J.O.: Functional data analysis. Wiley Online Library (2006)
8. Hong, Y., Davis, B., Marron, J., Kwitt, R., Niethammer, M.: Weighted functional boxplot with application to statistical atlas construction. In: Medical Image Computing and Computer-Assisted Intervention–MICCAI 2013. Springer (2013) 584–591

9. Sun, Y., Genton, M.G.: Functional boxplots. Journal of Computational and Graphical Statistics **20**(2) (2011)